

Approximating the long time average of the density operator: Diagonal ensembleAslı Çakan , J. Ignacio Cirac , and Mari Carmen Bañuls *Max-Planck-Institut für Quantenoptik, Hans-Kopfermann-Straße 1, 85748 Garching, Germany
and Munich Center for Quantum Science and Technology (MCQST), Schellingstraße 4, D-80799 Munich, Germany* (Received 12 November 2020; revised 25 February 2021; accepted 26 February 2021; published 8 March 2021)

For an isolated generic quantum system out of equilibrium, the long time average of observables is given by the diagonal ensemble, i.e., the mixed state with the same probability for energy eigenstates as the initial state but without coherences between different energies. In this work we present a method to approximate the diagonal ensemble using tensor networks. Instead of simulating the real time evolution, we adapt a filtering scheme introduced earlier [M. C. Bañuls, D. A. Huse, and J. I. Cirac, *Phys. Rev. B* **101**, 144305 (2020)] to this problem. We analyze the performance of the method on a nonintegrable spin chain, for which we observe that local observables converge towards thermal values polynomially with the inverse width of the filter.

DOI: [10.1103/PhysRevB.103.115113](https://doi.org/10.1103/PhysRevB.103.115113)**I. INTRODUCTION**

When an isolated quantum system is initialized in a pure state out of equilibrium, the unitary character of the evolution ensures that the state remains pure at any later times. However, if observations are restricted to a subsystem, thermalization may occur, that is, the rest of the system can act as a bath for the observed region [1,2]. More explicitly, if expectation values reach and remain close to a certain value for an extended period of time, one talks about equilibration [3–5]. And thermalization occurs if those values correspond to the expectation values at the thermal equilibrium state consistent with the energy of the system [1,2,6,7].

For a generic Hamiltonian with nondegenerate spectrum, the long time limit of time-averaged observables corresponds to the expectation value in the diagonal ensemble [8]. This mixed state, diagonal in the energy eigenbasis, can be seen as the average of the density operator of the system at all times. To decide whether the system can thermalize, it is thus enough to compare the expectation values in the diagonal ensemble to those in thermal equilibrium at the same energy. But while the thermal state of a local Hamiltonian can be efficiently approximated using tensor networks [9–11], simulating the out-of-equilibrium dynamics, and thus directly constructing the diagonal ensemble, is a much harder problem [12,13]. We notice that some numerical methods have been developed that can approximate the diagonal ensemble with some restrictions, such as exact diagonalization (limited to small systems) or the numerical linked cluster expansion

[14–16] (for which the expansion may fail to converge for some parameter choices, or initial states).

Generally speaking, integrable systems, due to their extensive number of conserved local quantities, do not thermalize but are instead argued to relax or equilibrate to the so-called generalized Gibbs ensemble [2,8,17,18], compatible with all the constraints. In contrast, nonintegrable systems are typically expected to thermalize [2,5,19–23]. It is thus especially interesting to identify nonintegrable systems that fail to do so, as the current interest in systems with many body localization [24–26], quantum scars [27], or disorder-free localization [28–30] makes evident. Nevertheless, the (absence of) thermalization of nonintegrable systems is hard to determine, since the applicability of analytical tools for such models is limited, and numerical simulations of out-of-equilibrium dynamics are restricted to small systems or short times.

In this paper, we present an alternative method to find a tensor network approximation to the diagonal ensemble, without resorting to the explicit simulation of the dynamics. We make use of a recently introduced filtering procedure [31], devised to prepare pure states with reduced energy variance, and show how it can be adapted to filter out the off-diagonal components of a density operator with respect to the energy basis.

More concretely, we apply to the initial density matrix a Gaussian operator that filters out large eigenvalues of the Hamiltonian commutator. In the limit of vanishing width of the Gaussian, the result will converge to the diagonal ensemble, in the most generic case, when there are no degeneracies in the spectrum. Notice that if there were degenerate energy levels, the procedure would leave untouched the coherences in the corresponding energy subspace, and thus would still lead to the correct limit of the time-averaged density operator. As described in [31], the filter can be approximated as a sum of Chebyshev polynomials, and its application to an initial vector can be numerically simulated using matrix product states [32,33] (MPS) methods, at least for moderate widths. Here we carry out these simulations for a spin chain

in the nonintegrable regime, and investigate how the values of local observables converge towards the thermal equilibrium. For comparison, we also consider an integrable instance of the same model, for which the observables may converge to different nonthermal values, depending on the initial state.

The rest of the paper is organized as follows. In Sec. II we review the filtering procedure and its application to the problem of the diagonal ensemble. We also discuss some properties of this specific application. Section III describes the main elements of our numerical simulations. Our results for the generic, nonintegrable case are shown in Sec. IV, where we discuss how the application of the approximate filter to this problem resembles and differs from that of reducing the energy variance, and analyze the convergence of local observables to their thermal values. The distinct behavior of an integrable instance is discussed in Sec. V. Finally, in Sec. VI we summarize our findings and discuss potential extensions of our work.

II. FILTERING THE DIAGONAL ENSEMBLE

Let us consider a system of size N governed by a (local) Hamiltonian H , and a pure initial state, which can be written in the energy eigenbasis as $|\Psi_0\rangle = \sum_n c_n |E_n\rangle$, with the normalization condition $\sum_n |c_n|^2 = 1$. We are interested in the long time average properties of the evolved state; i.e., given any physical observable $O = \sum_{n,m} O_{nm} |E_n\rangle\langle E_m|$, we want to compute

$$\lim_{T \rightarrow \infty} \frac{1}{T} \int dt \langle \Psi(t) | O | \Psi(t) \rangle = \sum_n |c_n|^2 O_{nn} = \text{tr}[\rho_D(\Psi_0)O], \quad (1)$$

where the first equality holds under the generic condition, which we assume in the following, that the spectrum is non-degenerate [34], and in the second one we have used the definition of the diagonal ensemble

$$\rho_D(\Psi_0) = \sum_n |c_n|^2 |E_n\rangle\langle E_n|. \quad (2)$$

If the system thermalizes, the diagonal expectation value $\langle O \rangle_D := \text{tr}(\rho_D O)$ will be equal to the expectation value in the thermal equilibrium state, $\rho_{th}(\beta) = e^{-\beta H} / \text{tr}(e^{-\beta H})$, that corresponds to the mean energy of the initial state. Thus, an approximation to the diagonal ensemble would allow us to probe whether a given state thermalizes or not.

In the energy eigenbasis, the density matrix for the initial state can be written as $\rho_0 = \sum_{n,m} c_n c_m^* |E_n\rangle\langle E_m|$. Filtering out the off-diagonal matrix elements in this basis will result in the diagonal ensemble (2). We thus define an (unnormalized) Gaussian filter which acts on the mixed state as a superoperator,

$$F_\sigma[\rho] := e^{-\hat{H}_C^2/2\sigma^2}[\rho], \quad (3)$$

where \hat{H}_C is the commutator with the Hamiltonian, i.e., $\hat{H}_C[\rho] = H\rho - \rho H$. Notice that F_σ is a completely positive trace preserving map, i.e., a quantum channel. The effect of this filter is to suppress the off-diagonal matrix elements corresponding to pairs of states with different energies. As the width σ is reduced, and, for a generic, nondegenerate

Hamiltonian, the application of the filter will converge to the desired result

$$F_\sigma[\rho_0] \xrightarrow{\sigma \rightarrow 0} \rho_D(\Psi_0).$$

Notice that the filter would not affect the density operator components in a degenerate energy subspace. Thus, if the Hamiltonian has degenerate levels, the limit of the procedure is block diagonal, corresponding to the long time limit of the time average of the evolved state.

Mapping the basis operators to vectors [35] as $|E_n\rangle\langle E_m| \rightarrow |E_n E_m\rangle$, we can write the density matrix as a vector of dimension 2^{2N} , on which the filter acts as a linear operator, and the problem becomes formally analogous to the energy filters used in [31,36–38].

In this representation, the commutator corresponds to the linear operator $\hat{H}_C = H \otimes \mathbb{1} - \mathbb{1} \otimes H^T$, which, if H is local, is also a local Hamiltonian with eigenvectors $|E_n E_m\rangle$ and corresponding eigenvalues $E_n - E_m$, for $n, m = 1, \dots, 2^N$. We can then apply the filtering procedure for reducing the energy variance from a state with given mean energy described in [31]. For a product initial state $|\Psi_0\rangle$, the (vectorized) initial density matrix $|\rho_0\rangle = |\Psi_0\rangle \otimes |\Psi_0\rangle$ is also a product, and the scenario is very similar to the one discussed in that reference.

With respect to the Hamiltonian \hat{H}_C , any physical state has mean value $\langle \rho_0 | \hat{H}_C | \rho_0 \rangle = \text{tr}(\rho_0^\dagger [H, \rho_0]) = 0$. The filter (3) preserves this property of the initial state while it reduces the corresponding (effective energy) variance, $\langle \rho | \hat{H}_C^2 | \rho \rangle = -\text{tr}([H, \rho]^2)$, which measures precisely the off-diagonal part of the density operator in the energy basis.

A. Chebyshev approximation of the filter

Formally, this filtering procedure is analogous to the one described in [31], and some of the properties can be directly translated to the current case. In particular, the Gaussian filter F_σ can be approximated by a series of Chebyshev polynomials.

Any piecewise continuous function $f(x)$ defined in the interval $x \in [-1, 1]$ can be approximated by a linear combination of the M lowest-degree Chebyshev polynomials [39]. In particular, the corresponding series for the delta function truncated to order M (and improved using the kernel polynomial method) is known to approximate a Gaussian of width $\sqrt{\pi}/M$. We can thus use such series to order $M \propto N/\sigma$ to approximate the Gaussian filter F_σ . This sum has the form

$$Q_M := \sum_{m=0}^{\lfloor M/2 \rfloor} (-1)^m \frac{2 - \delta_{m0}}{\pi} \gamma_{2m}^M T_{2m}(\alpha \hat{H}_C), \quad (4)$$

where α is a rescaling constant to ensure that the spectrum of $\alpha \hat{H}_C$ lies strictly within the interval $[-1, 1]$. We use $H_C = \alpha \hat{H}_C$ for the rescaled Hamiltonian commutator in the rest of the paper. $T_m(x)$ is the m -th Chebyshev polynomial of the first kind, defined by the recurrence relations $T_0(x) = 1$, $T_1(x) = x$, and $T_{m+1}(x) = 2xT_m(x) - T_{m-1}(x)$, and γ_m^M are the Jackson kernel coefficients [39],

$$\gamma_m^M = \frac{(M - m + 1) \cos \frac{\pi m}{M+1} + \sin \frac{\pi m}{M+1} \cos \frac{\pi}{M+1}}{M + 1}. \quad (5)$$

We will denote the result of applying the series expansion to order M as

$$|\rho_M\rangle := Q_M|\rho_0\rangle. \quad (6)$$

Notice that this vector has a different normalization than $|\rho_\sigma\rangle$, because the sum in Q_M approximates a normalized Gaussian distribution, unlike F_σ from (3).

The off-diagonal width of the operator ρ_M is determined by the corresponding variance of H_C as

$$\delta^2 := \frac{\langle \rho_M | H_C^2 | \rho_M \rangle}{\langle \rho_M | \rho_M \rangle}. \quad (7)$$

B. Properties of the diagonal filter

Notice that the filtering procedure described so far is general, as it does not make any assumption on the spatial dimension of the problem. In the following we will focus on a one-dimensional problem, for which we can use tensor networks in order to obtain numerical approximations. As in [31], we can use matrix product state (MPS) techniques [32,33] to simulate the application of this filter to an initial state. In this way we construct a matrix product operator (MPO) [40–42] approximation to the filtered ensemble. Also here, for large system sizes and narrow filters, the required bond dimension for the approximation can be bounded as $D \lesssim c' \sqrt{N} D_0^{1/\delta}$, where c' and D_0 are $O(1)$ constants. Accordingly, the expression for the entanglement entropy,

$$S \lesssim k/\delta + \log \sqrt{N} + \text{const}, \quad (8)$$

corresponds now to a bound for the operator space entanglement entropy (OSSE) [43].

The spectrum of H_C exhibits, however, an exponential degeneracy in the subspace of eigenvalue zero, which imposes a significant difference. For each eigenstate $|E_n\rangle$ of H , $|E_n E_n\rangle$ is an eigenstate of H_C with zero eigenvalue. Thus, even if the spectrum of H is nondegenerate and even if it fulfills the stronger assumption of nondegenerate gaps, the “zero energy” subspace of H_C is always exponentially degenerate.

Hence the target diagonal ensemble states could in principle have arbitrarily small OSSE, even with vanishing width σ (an extreme case would be the maximally mixed state, with zero OSSE). This is in contrast to the Hamiltonian filtering, where the limit would generically have thermal (i.e., volume law) entanglement. Even if we expect that the general relations between energy fluctuations and entropy or bond dimension demonstrated in [31] still hold during the main part of the filtering procedure, eventually, as the width becomes negligible and the procedure converges to the diagonal ensemble, the OSSE can converge to a nongeneric value that will depend on the initial state.

The scenario we discuss here also exhibits another fundamental difference regarding physical observables. For a local operator O , the expectation value is computed as

$$\frac{\text{tr}(O\rho)}{\text{tr}\rho} = \frac{\langle O | \rho \rangle}{\langle \mathbb{1} | \rho \rangle},$$

where $|O\rangle$ and $|\mathbb{1}\rangle$ are respectively the vectorized observable and identity operators.

As an overlap between two vectors, this is a global quantity, and no longer local in space. Therefore, the considerations in [31] about the minimal entanglement of a subregion required for local observables to converge to thermal values do not immediately apply here.

C. Convergence of the off-diagonal components

The initial state is given by a physical density operator, normalized in trace, $\text{tr}\rho_0 = 1$, and also Frobenius norm, $\langle \rho_0 | \rho_0 \rangle = \text{tr}\rho_0^2 = 1$. The filter (3) preserves the former, but not the latter. Instead, the norm of the filtered vector $|\rho_\sigma\rangle$ indicates the magnitude of the remaining off-diagonal components.

The state resulting from the application of the original Gaussian filter F_σ on ρ_0 can be written as a sum of two mutually orthogonal components,

$$|\rho_\sigma\rangle = |\rho_D\rangle + \sum_{n,m \neq n} c_n c_m^* e^{-(E_n - E_m)^2 / (2\sigma^2)} |E_n E_m\rangle. \quad (9)$$

The first term is precisely the diagonal ensemble, and the second one includes all off-diagonal components of the density operator. Denoting them by $|\Delta\rho\rangle := |\rho_\sigma\rangle - |\rho_D\rangle$, the (Frobenius) norm of the off-diagonal components is

$$\langle \Delta\rho | \Delta\rho \rangle = \sum_{n,m \neq n} |c_n|^2 |c_m|^2 e^{-(E_n - E_m)^2 / \sigma^2}. \quad (10)$$

The magnitude of these components may be estimated using simple arguments. We consider as initial state ρ_0 a pure product state, for which the energy distribution, given by $|c_n|^2$, is peaked around the mean energy $E_{\rho_0} = \text{tr}(H\rho_0)$, and has variance $O(N)$. For large systems, this distribution behaves as a Gaussian [44] and we can approximate the norm of the vector $|\rho_\sigma\rangle$ by a double integral over energies, from which we obtain

$$\langle \rho_\sigma | \rho_\sigma \rangle \sim \frac{\sigma}{\sqrt{N}}. \quad (11)$$

The norm of the diagonal component, equivalent to the inverse participation ratio of the initial state, $\langle \rho_D | \rho_D \rangle = \sum_n |c_n|^4$ is independent of σ . Typically, the number of energy eigenstates contributing to the sum will be exponentially large in the system size, unless the mean energy of the initial state E_ρ corresponds to a region of exponentially small density of states. To see this, we can take again into account the aforementioned distribution of the weights for our initial states, and the fact that for large systems the density of states approaches also a Gaussian distribution [44,45]. The inverse participation ratio then decreases exponentially with the system size,

$$\langle \rho_D | \rho_D \rangle \sim 2^{-N}. \quad (12)$$

Unless the width of the filter is exponentially small in N , the norm of the filtered state is dominated by the off-diagonal component, and we expect both of them to decrease proportionally to the width, for fixed size N , according to (11). Notice nevertheless that a bound on the (Frobenius) norm of $|\Delta\rho\rangle$ is not enough to extract conclusions about the convergence of physical observables, a question that we explore numerically in Sec. IV.

III. SETUP FOR THE NUMERICAL SIMULATIONS

We use numerical simulations to explore some of the questions in the previous section. In particular, we investigate whether the diagonal ensemble can be approximated by a MPO, and how the physical observables approach the diagonal expectation values as we filter out the off-diagonal matrix elements of the density matrix.

A. MPS approximation of the ensemble

We use matrix product operators (MPO) [40,41,46] to represent the density operators corresponding to the initial and filtered states. Once vectorized, they are represented by MPS with double physical indices, which can be manipulated using standard tensor network methods [32,33,47,48].

We find a MPS approximation for the action of the filter (4) on a given initial state. The method is completely analogous to the one presented in [31] for filtering out energy fluctuations, with the only difference that here the effective Hamiltonian is the commutator superoperator H_C acting on the vectorized density matrices. For a local Hamiltonian H , the commutator H_C can also be written as a MPO.

As in [31,38,49–52] we can then take advantage of the fact that we do not need the full polynomials $T_m(H_C)$, which in our case are operators acting on a 2^{2N} dimensional vector space, but only the vectors resulting from their action on the initial state $T_m(H_C)|\rho_0\rangle$. The latter satisfy the same recurrence relation as the polynomials and can be computed with lower computational cost.

B. Model and initial states

We focus our study in the Ising spin chain with both longitudinal and transverse fields,

$$H_{\text{Ising}} = J \sum_i \sigma_z^{[i]} \sigma_z^{[i+1]} + g \sum_i \sigma_x^{[i]} + h \sum_i \sigma_z^{[i]}. \quad (13)$$

If either $g = 0$ or $h = 0$, the model becomes exactly solvable. For the remaining of this section we focus on the generic, non-integrable case. We choose parameters $(J, g, h) = (1, -1.05, 0.5)$, far from the integrability limit.

As initial states we consider product states in which all spins are aligned in the same direction for both models. We denote such states by the direction in which the spins are aligned, e.g., $|X\pm\rangle = 2^{-N/2}(|0\rangle \pm |1\rangle)^{\otimes N}$, $|Y\pm\rangle = 2^{-N/2}(|0\rangle \pm i|1\rangle)^{\otimes N}$, $|Z+\rangle = |0\rangle^{\otimes N}$, and $|Z-\rangle = |1\rangle^{\otimes N}$.

IV. NUMERICAL RESULTS

We have applied the procedure described in the previous section to system sizes $N \in \{20, 60\}$, using MPS with bond dimensions $100 \leq D \leq 1500$. Additionally, we cross-check results for small system sizes $N \leq 20$ which can be explored with exact diagonalization.

A. Scaling

We expect the off-diagonal width δ of our simulations to follow the scaling predicted in Ref. [31], namely $\delta^2 \propto 1/M^2$, for large enough number of terms in the approximation of the filter, and provided that the truncation error is not

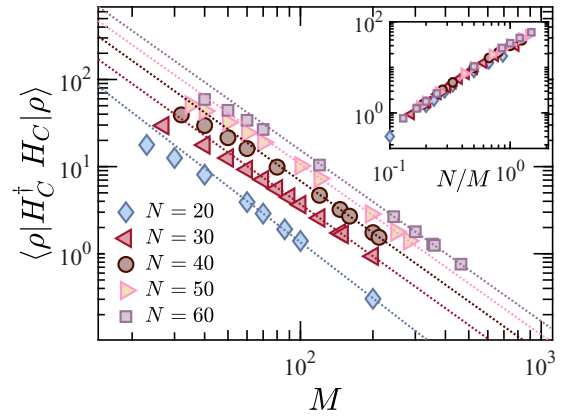


FIG. 1. Scaling of the variance $\delta^2 = \langle \rho_M | H_C^\dagger H_C | \rho_M \rangle$, as a function of the Chebyshev truncation parameter M for different system sizes $N = 20$ –60 with bond dimension $D = 1000$ and initial state $|X+\rangle$. Except for the smallest values of M , we find that our results scale with the expected [31] $\delta^2 \propto 1/M^2$.

significant. Thus, the decrease of the width with M provides us with a check that our simulations are in the expected regime. Figure 1 shows that this is indeed the case. The figure shows that, for all system sizes, the converged data are well described by a power law fit $\delta^2 \propto M^{-\alpha}$ (dotted lines) with exponents $-2.13, -1.98, -1.97, -1.95, -1.96$ for $N = 20, 30, 40, 50, 60$, respectively.

A further check is provided by the norm of the filtered state $|\rho_\sigma\rangle$. As described in Sec. II C, $\langle \rho_\sigma | \rho_\sigma \rangle$ should decrease as the inverse off-diagonal width. Since our algorithm applies the normalized filter (4), $Q_M \sim \frac{1}{\sqrt{2\pi\sigma^2}} F_\sigma$, we expect, for the proper values of M and σ ,

$$\langle \rho_M | \rho_M \rangle \sim \frac{1}{\sigma\sqrt{N}}. \quad (14)$$

To directly probe this relation, we plot the vector norm of our resulting state in Fig. 2, for system sizes $N = 20$ –60, and find that our data agree well with this prediction, except for the smallest values of M .

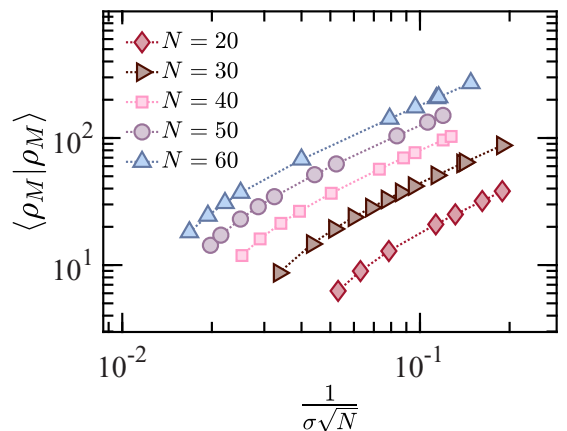


FIG. 2. Relation between vector norm of off-diagonal components and inverse off-diagonal width for system sizes $N = 20$ –60 and bond dimension, $D = 1000$, starting with initial state $|X+\rangle$.

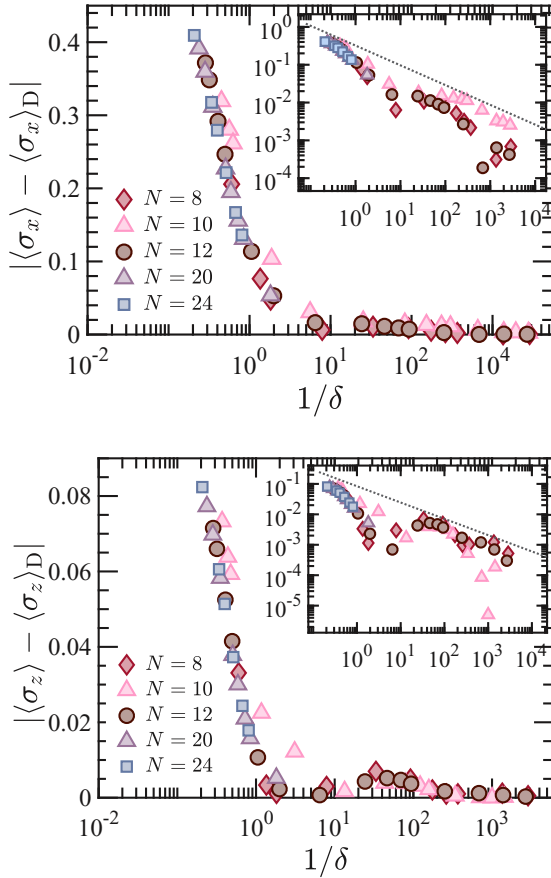


FIG. 3. Absolute error in local observables σ_x (upper) and σ_z (lower figure) between exact diagonal ensemble values and Chebyshev filter results as a function of inverse off-diagonal width for system sizes $N = 8, 10, 12, 20$, and 24 with the initial state $|X+\rangle$. The insets indicate the log-log plots of the corresponding figures, where we show the upper bounds with the straight dotted lines. The slope for σ_x is -0.52 and it is -0.53 for σ_z .

B. Convergence of local observables

As the filtered state approaches the diagonal ensemble, so will the values of physical observables. If the state thermalizes, such a limit will agree with the thermal value corresponding to the initial energy, and thus comparing this to the converged values can be used to probe thermalization of the system. Here we are interested in the rate of convergence of the physical expectation values.

For the problem of reducing the energy variance of a pure state, it has been predicted that for chaotic systems [53] a polynomial decrease of the variance with the system size is required for all local observables to converge to their thermal values. In Ref. [31] it was numerically observed for model (13) that an energy variance decreasing as $1/\log N$ or faster was sufficient for convergence in the thermodynamic limit. But as discussed in Sec. II, these conclusions do not need to apply in our case, because the expectation value in the mixed state does not have the same local structure. We thus explore this question numerically by studying the local x and z magnetizations in the middle of the chain, $\mathcal{O} = \sigma_{x,z}^{\lfloor N/2 \rfloor}$, and analyzing how the expectation values vary as the width

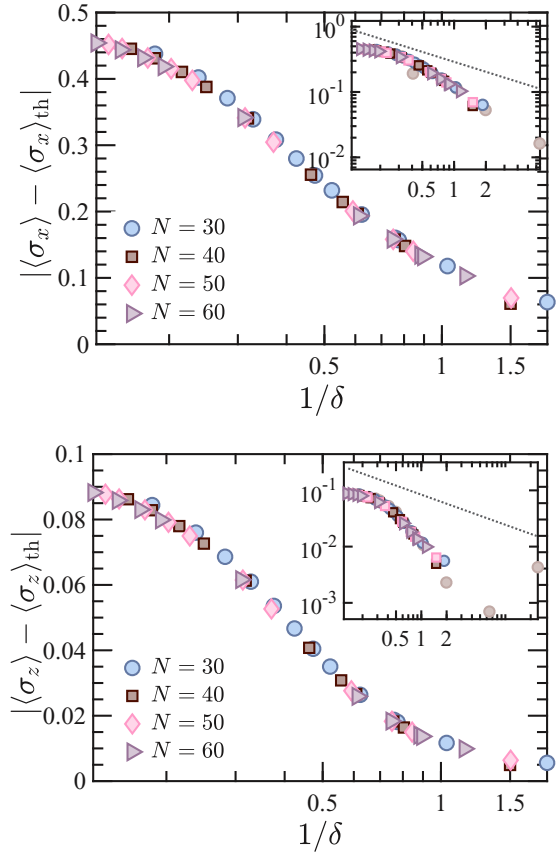


FIG. 4. Absolute error in local observables σ_x (upper) and σ_z (lower figure) between thermal values and numerical results based on a Chebyshev filter as a function of inverse off-diagonal width for system sizes $N = 30-60$ with the initial state $|X+\rangle$. The insets indicate the log-log plots of the corresponding figures, where we add the upper bounds with the dotted lines and the data points belong to $N = 12$ with lighter color as reference values taken from Fig. 3.

of the filter decreases. For systems of size $N \leq 12$ we can compute the action of the filter exactly for any width, while for larger systems, up to $N \leq 60$, we run MPS simulations up to the narrowest filter widths that we can reliably reach with a maximum bond dimension $D = 1000$.

For small systems, $N \leq 24$, we can compare the filtered values to the exact compute the exact magnetizations in the diagonal ensemble. For larger systems we do not have access to either the evolved state at long times or the exact diagonal ensemble, but we can approximate the thermal ensemble corresponding to the initial energy using MPO [40,41,54]. For the cases we study, there are analytical and numerical arguments in favor of thermalization [38,55], such that the thermal expectation values should be very close to the diagonal ones. Thus, for our analysis it is enough to use the thermal value as reference, since we are only exploring the variation of the expectation values, but our simulations for large systems do not reach full convergence (see Sec. IV D for a more detailed discussion of the numerical errors).

We plot the results for small and large system sizes in Figs. 3 and 4 for initial state $|X+\rangle$, and in Figs. 5 and 6 for initial state $|Z+\rangle$. In all cases we represent the absolute value

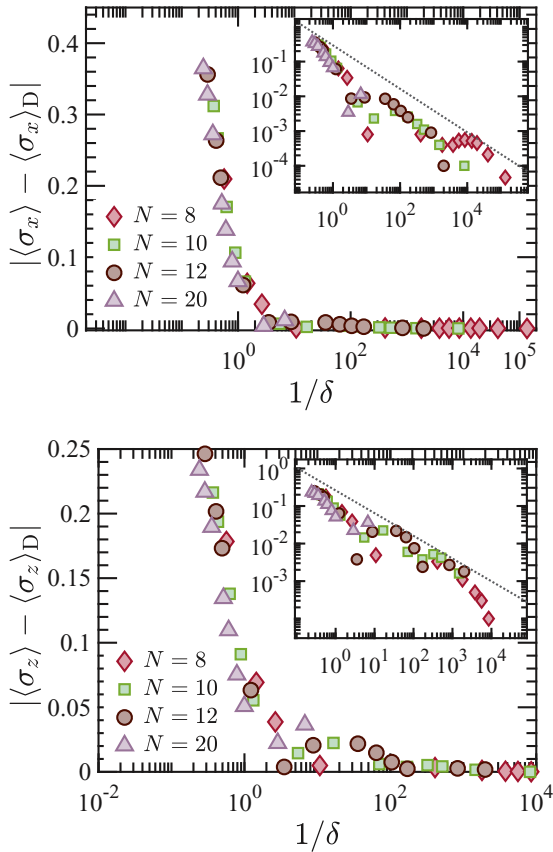


FIG. 5. Absolute error in local observables σ_x (upper) and σ_z (lower figure) between exact diagonal ensemble values and Chebyshev filter results, as a function of inverse off-diagonal width for system sizes $N = 8, 10, 12$, and 20 with the initial state $|Z+\rangle$. The insets indicate the log-log plots of the corresponding figures, where we show the upper bounds with the grey dotted lines. The slope for σ_x is $-0.62(63)$ and it is $-0.60(47)$ for σ_z .

of the difference between the expectation values in $|\rho_M\rangle$ and the diagonal (thermal, for large systems) values as a function of the off-diagonal width δ . In all cases, i.e., for the different initial states and different sizes, we observe that this absolute error, which is given exclusively by the off-diagonal part of ρ_M , decreases at least as fast as $1/\sqrt{\delta}$ (see insets). Moreover, the figures show that curves for different system sizes practically collapse on top of each other.

C. Entropy

Since we start with a product state $|\rho_0\rangle$ and evolve it with a local Hamiltonian H_C , the same arguments used in the case of pure states [31,56] then imply that the OSEE can be bounded as a function of the off-diagonal width and the system size as given in Eq. (8).

Figure 7 (upper panel) shows that, indeed, the evolution of the OSEE while filtering out the off-diagonal components of the state satisfies a similar bound. The plot shows the OSEE corresponding to the middle cut of the approximate filtered state ρ_M , as a function of the system size, for simulations in which the number of Chebyshev terms was chosen as different functions of the size $M = f(N)$, corresponding to

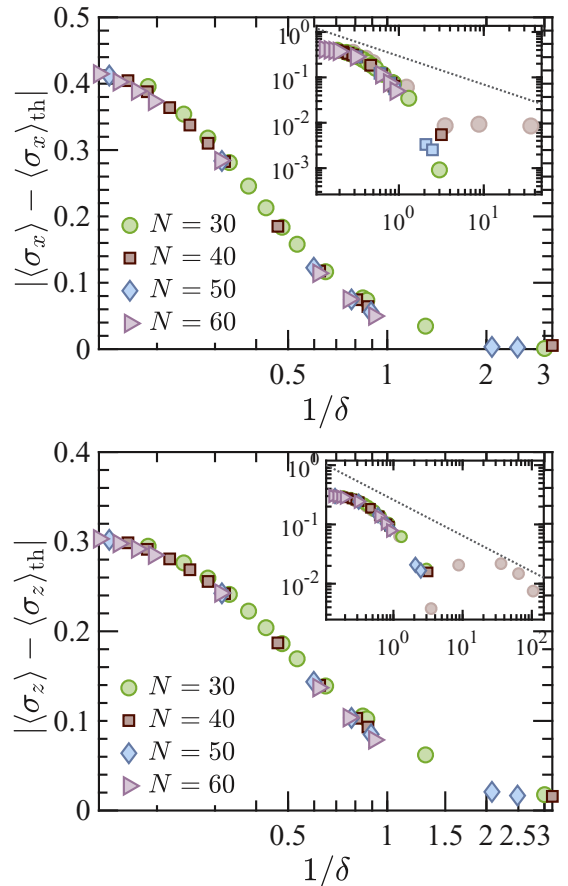


FIG. 6. Absolute error in local observables σ_x (upper) and σ_z (lower figure) between thermal values and numerical results based on a Chebyshev filter as a function of inverse off-diagonal width for system sizes $N = 30-60$ with the initial state $|Z+\rangle$. The insets indicate the log-log plots of the corresponding figures, where we put the upper bounds with the dotted lines and the data points belong to $N = 12$ with lighter color as reference values taken from Fig. 5.

a width $\delta(N) \propto 1/M$. We observe that for $M \propto \sqrt{N}$, which corresponds to $\delta \propto \sqrt{N}$, the OSEE does not grow with the system size, while for $M \propto N$ or $M \propto N \log N$ (correspondingly $\delta \sim \text{const}$ or $\delta \propto 1/\log N$), it increases as $\log N$. For faster growing $M \propto N^2$, also the increase in entropy is faster (compatible with it growing at most as N , as predicted by the argument in [31]).

The asymptotic universal scaling of the entropy can be appreciated more explicitly in Fig. 7 (lower), which shows that $2^S \propto \sqrt{N}(D_0^{1/\delta} - 1)$ for all system sizes $N \geq 20$ with a constant $D_0 = 2.76$.

The limit of the filtering procedure when the width vanishes is a mixed state in the exponentially degenerate null space of H_C . This subspace supports states with zero OSEE (e.g., the maximally mixed state), and thus the final OSEE is not generic, but will be determined by the initial state, in contrast to the case of pure state filtering, where we could generically expect that the entanglement entropy converges to a thermal volume law. We can explore how the limit value is approached during the filtering by analyzing the results for small systems, as shown in Fig. 8. As illustrated in the figure

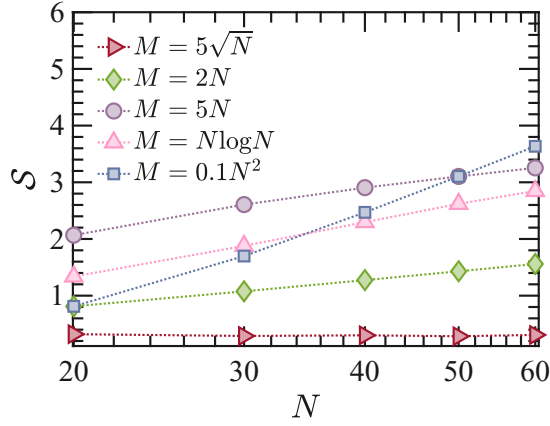


FIG. 7. Upper figure: Operator space entanglement entropy of the half chain as a function of logarithm of the system size, N , with different truncation numbers of Chebyshev filter, $M = f(N)$, and bond dimension, $D = 1000$, for initial state $|X+\rangle$. Our data show that the entropy grows with $\log N$ in all cases except that the line for $M = 5\sqrt{N}$ stays constant. Lower figure: Behavior of the exponential of the entropy as predicted by Ref. [31] that we have shown in Eq. (8). The dotted line indicates the linear fit where all data points locate on the same line as expected for large system sizes. D_0 from fitting the data for all system size is $2.76(40)$ and the slope of the fit is 1.

for different initial states and sizes $N \leq 12$, the entropy grows with $1/\delta$ for moderate widths, but it reaches a maximum after a certain point, and then decreases towards the diagonal value. If we examine how this final value depends on the system

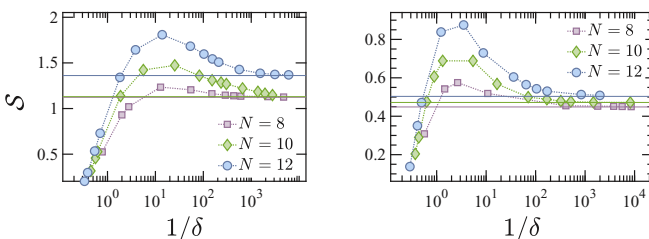


FIG. 8. Relation between entropy and logarithm of $1/\delta$ based on exact calculation for $N = 8, 10, 12$ with initial state, $|X+\rangle$ (left) and $|Z+\rangle$ (right figure).

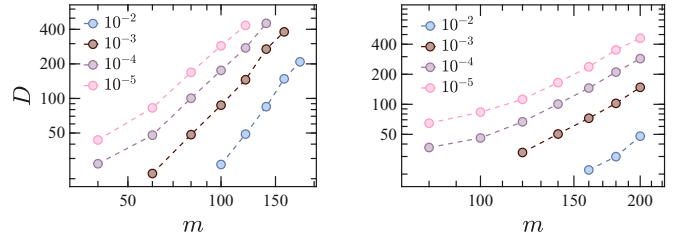


FIG. 9. Scaling of the bond dimension required to keep a constant precision in the MPS approximation of $T_m(H_C)|\rho_0\rangle$, as a function of the degree m for various values of the truncation error, 10^{-2} , 10^{-3} , 10^{-4} , 10^{-5} , and system sizes $N = 20$ (left) and $N = 30$ (right) for $D = 500$.

size, we observe that in all the cases studied the diagonal OSEE increases almost linearly with the size, although the values change considerably from one state to another, where the slope of each initial state is $0.06(78)$, $0.89(17)$, $0.02(37)$ for $|X+\rangle$, $|Y+\rangle$, $|Z+\rangle$, respectively.

D. Error analysis

In our strategy, for a fixed order M of the Chebyshev expansion, the main source of error is the truncation error, namely approximating the action of each Chebyshev polynomial on the initial state by a MPS with limited bond dimension. We can quantify this error for a given order m using as reference the best approximation found for the corresponding term $T_m(H_C)|\rho_0\rangle$ (in our case, with $D = 1000$) and comparing it to its truncated versions with smaller bond dimensions. In this way we can extract the bond dimension required for fixed precision. In previous works that used MPS approximations of Chebyshev series [38,49–52] it was observed that the required bond dimension for such terms increases polynomially with the degree m . Our results, illustrated in Fig. 9, seem to agree with such behavior, except for the smallest values of m . We have also observed, as in the recent work [38], that for fixed m the bond dimension required to maintain constant truncation error in $T_m(H_C)|\rho_0\rangle$ gets smaller for larger system sizes. Notice, however, that for larger systems, also polynomials of higher degree will be required to attain a constant width δ , since, as discussed in Sec. II A, the order of the expansion scales as $M \propto N/\delta$.

V. INTEGRABLE CASE

The results in section IV B are consistent with the generic expectation that, for nonintegrable cases, the values of local observables in the diagonal ensemble agree with those in thermal equilibrium. But the presence of local conserved quantities imposes constraints on the equilibration of observables. Thus, for integrable models, long time averages are not expected to agree with the thermal ensemble. Instead, the system could in such cases converge to a generalized Gibbs ensemble [8] compatible with all conserved quantities.

We expect that, as the width of the filter decreases, our method approximates the actual time averaged state in the limit of infinite time. Hence local observables can converge to values that differ from thermal equilibrium. In order to probe this case, we have applied the method to an integrable choice

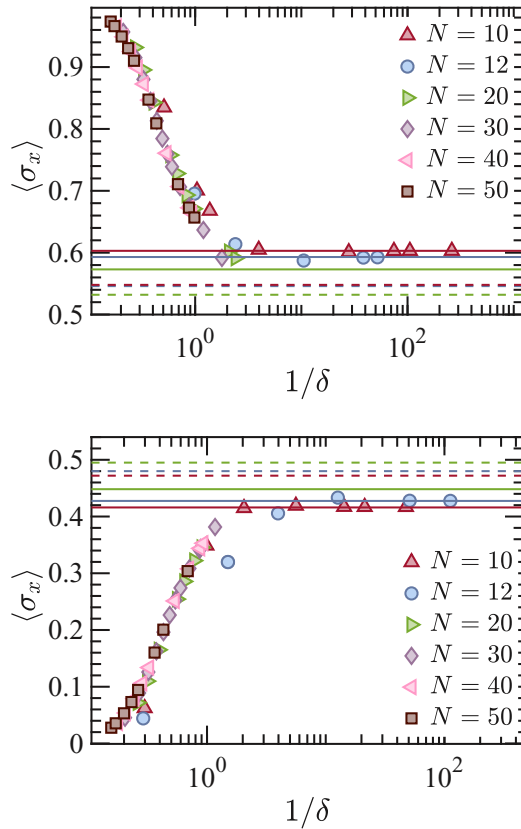


FIG. 10. Expectation value of local observables σ_x at the middle of the chain based on Chebyshev filter simulations for initial states $|X+\rangle$ (upper) and $|Z+\rangle$ (lower figure) as a function of inverse off-diagonal width for system sizes $N = 10$ – 50 . Red, blue, and green solid lines indicate the long time average values for $N = 10, 12, 20$ respectively. Red, blue, and green dashed lines indicate the thermal values for the same system sizes $N = 10, 12, 20$ respectively, belonging to the same color map in the legend.

of parameters in Eq. (13), namely $(J, g, h) = (1, 1.05, 0.)$, for various translationally invariant product states. We have simulated system sizes up to $N = 50$, with bond dimension up to $D = 1000$.

The scaling of variance and entropy with the filter width in the integrable case does not substantially differ from those described in Secs. IV A and IV C. However, local observables can exhibit qualitative differences, as illustrated in Fig. 10.

Figure 10 shows the convergence of a local observable $\langle \sigma_x \rangle$ at the middle of the chain as a function of the inverse width $1/\delta$, for two different initial states $|X+\rangle$ and $|Z+\rangle$. In both cases, the limit of the time averaged observable noticeably differs from the thermal value, as we have checked using exact diagonalization for system sizes $N \leq 20$. Applying our algorithm to these and also larger system sizes indeed suggests

convergence of the observable to values that are distinct from thermal equilibrium (indicated by dashed horizontal lines).

VI. DISCUSSION

We have presented a method to approximate the diagonal ensemble corresponding to a quantum many-body state. By applying a Gaussian filter to the density operator, the off-diagonal components in the energy basis are suppressed and, in the limit of vanishing filter width, the result converges to the ensemble that represents the long time average of the time evolved state. For a Hamiltonian with nondegenerate spectrum, this is the diagonal ensemble.

Numerically, the filter can be approximated by a Chebyshev polynomial series, and applied using MPS standard techniques, in an analogous manner to what was already described in Ref. [31] for an energy filter. In our case, we obtain a MPO approximation to the filtered ensemble.

The method allows us to treat larger systems than exact diagonalization. However, our results for small systems indicate that the operator space entanglement entropy of the diagonal ensemble scales as a volume law, which limits the system sizes for which the MPO can provide a reliable approximation. Still, we are able to simulate the effect of filters with moderate off-diagonal width and to analyze the convergence of local observables towards the thermal equilibrium.

We have applied this method to a nonintegrable spin chain and several out-of-equilibrium product initial states for system sizes up to $N = 60$. We have numerically observed that local observables converge towards their thermal values as a power of the inverse off-diagonal width. Remarkably, this behavior is mostly independent of the system size. Even for moderate off-diagonal widths, the method provides in this way insight beyond exact diagonalization. In the future, it can be thus used to explore other one-dimensional models.

It is worth noticing that our procedure does not directly target the diagonal ensemble, but the limit of the time-averaged state. In an integrable case this can be a generalized Gibbs ensemble, and differ considerably from the thermal equilibrium one (see, e.g., [14,15,57]). For an integrable instance of the model, we have explicitly shown how local observables in the filtered state can indeed converge to values far from thermal equilibrium. A detailed analysis of integrable cases requires, however, more precise simulations than the ones shown here, and is left for future investigation.

ACKNOWLEDGMENTS

This work was partially funded by the Deutsche Forschungsgemeinschaft (DFG, German Research Foundation) under Germany's Excellence Strategy, EXC-2111–390814868, and by the European Union through the ERC grant QUENOCOBA, ERC-2016-ADG (Grant No. 742102).

- [1] J. M. Deutsch, *Phys. Rev. A* **43**, 2046 (1991).
 [2] M. Rigol, V. Dunjko, and M. Olshanii, *Nature (London)* **452**, 854 (2008).
 [3] M. Srednicki, *J. Phys. A: Math. Gen.* **32**, 1163 (1999).

- [4] L. Masanes, A. J. Roncaglia, and A. Acín, *Phys. Rev. E* **87**, 032137 (2013).
 [5] C. Gogolin and J. Eisert, *Rep. Prog. Phys.* **79**, 056001 (2016).
 [6] M. Srednicki, *Phys. Rev. E* **50**, 888 (1994).

- [7] J. Berges and J. Cox, *Phys. Lett. B* **517**, 369 (2001).
- [8] M. Rigol, V. Dunjko, V. Yurovsky, and M. Olshanii, *Phys. Rev. Lett.* **98**, 050405 (2007).
- [9] M. B. Hastings, *Phys. Rev. B* **73**, 085115 (2006).
- [10] A. Molnar, N. Schuch, F. Verstraete, and J. I. Cirac, *Phys. Rev. B* **91**, 045138 (2015).
- [11] T. Kuwahara, Álvaro M. Alhambra, and A. Anshu, *Phys. Rev. X* (to be published), [arXiv:2007.11174](https://arxiv.org/abs/2007.11174).
- [12] T. J. Osborne, *Phys. Rev. Lett.* **97**, 157202 (2006).
- [13] N. Schuch, M. M. Wolf, K. G. H. Vollbrecht, and J. I. Cirac, *New J. Phys.* **10**, 033032 (2008).
- [14] M. Rigol, *Phys. Rev. Lett.* **112**, 170601 (2014).
- [15] M. Rigol, *Phys. Rev. E* **90**, 031301 (2014).
- [16] K. Mallayya and M. Rigol, *Phys. Rev. E* **95**, 033302 (2017).
- [17] M. Cramer, C. M. Dawson, J. Eisert, and T. J. Osborne, *Phys. Rev. Lett.* **100**, 030602 (2008).
- [18] L. D'Alessio, Y. Kafri, A. Polkovnikov, and M. Rigol, *Adv. Phys.* **65**, 239 (2016).
- [19] C. Kollath, A. M. Läuchli, and E. Altman, *Phys. Rev. Lett.* **98**, 180601 (2007).
- [20] S. R. Manmana, S. Wessel, R. M. Noack, and A. Muramatsu, *Phys. Rev. Lett.* **98**, 210405 (2007).
- [21] A. Flesch, M. Cramer, I. P. McCulloch, U. Schollwöck, and J. Eisert, *Phys. Rev. A* **78**, 033608 (2008).
- [22] M. Moeckel and S. Kehrein, *Phys. Rev. Lett.* **100**, 175702 (2008).
- [23] M. Rigol, *Phys. Rev. Lett.* **103**, 100403 (2009).
- [24] A. C. Cassidy, D. Mason, V. Dunjko, and M. Olshanii, *Phys. Rev. Lett.* **102**, 025302 (2009).
- [25] L. F. Santos and M. Rigol, *Phys. Rev. E* **81**, 036206 (2010).
- [26] D. A. Abanin, E. Altman, I. Bloch, and M. Serbyn, *Rev. Mod. Phys.* **91**, 021001 (2019).
- [27] C. J. Turner, A. A. Michailidis, D. A. Abanin, M. Serbyn, and Z. Papić, *Phys. Rev. B* **98**, 155134 (2018).
- [28] Z. Papić, E. M. Stoudenmire, and D. A. Abanin, *Ann. Phys. (NY)* **362**, 714 (2015).
- [29] A. Smith, J. Knolle, D. L. Kovrizhin, and R. Moessner, *Phys. Rev. Lett.* **118**, 266601 (2017).
- [30] M. Schulz, C. A. Hooley, R. Moessner, and F. Pollmann, *Phys. Rev. Lett.* **122**, 040606 (2019).
- [31] M. C. Bañuls, D. A. Huse, and J. I. Cirac, *Phys. Rev. B* **101**, 144305 (2020).
- [32] F. Verstraete, V. Murg, and J. Cirac, *Adv. Phys.* **57**, 143 (2008).
- [33] U. Schollwöck, *Ann. Phys. (NY)* **326**, 96 (2011), January 2011 Special Issue.
- [34] If this condition is not fulfilled, ρ_D should be replaced by a block-diagonal operator, where each block corresponds to a different energy subspace, with the same matrix elements as in the initial state.
- [35] M.-D. Choi, *Linear Algebra Appl.* **10**, 285 (1975).
- [36] S. Lu, M. C. Bañuls, and J. I. Cirac, [arXiv:2006.03032](https://arxiv.org/abs/2006.03032).
- [37] Y. Ge, J. Tura Brugués, and J. Cirac, *J. Math. Phys.* **60**, 022202 (2019).
- [38] Y. Yang, S. Iblisdir, J. I. Cirac, and M. C. Bañuls, *Phys. Rev. Lett.* **124**, 100602 (2020).
- [39] A. Weiße, G. Wellein, A. Alvermann, and H. Fehske, *Rev. Mod. Phys.* **78**, 275 (2006).
- [40] F. Verstraete, J. J. García-Ripoll, and J. I. Cirac, *Phys. Rev. Lett.* **93**, 207204 (2004).
- [41] M. Zwolak and G. Vidal, *Phys. Rev. Lett.* **93**, 207205 (2004).
- [42] B. Pirvu, F. Verstraete, and G. Vidal, *Phys. Rev. B* **83**, 125104 (2011).
- [43] T. c. v. Prosen and I. Pižorn, *Phys. Rev. A* **76**, 032316 (2007).
- [44] M. Hartmann, G. mahler, and O. Hess, *Lett. Math. Phys.* **68**, 103 (2004).
- [45] J. P. Keating, N. Linden, and H. J. Wells, *Commun. Math. Phys.* **338**, 81 (2015).
- [46] B. Pirvu, V. Murg, J. I. Cirac, and F. Verstraete, *New J. Phys.* **12**, 025012 (2010).
- [47] R. Orús, *Ann. Phys. (NY)* **349**, 117 (2014).
- [48] P. Silvi, F. Tschirsich, M. Gerster, J. Jünemann, D. Jaschke, M. Rizzi, and S. Montangero, *SciPost Phys. Lect. Notes*, 8 (2019), doi: [10.21468/SciPostPhysLectNotes.8](https://doi.org/10.21468/SciPostPhysLectNotes.8).
- [49] A. Holzner, A. Weichselbaum, I. P. McCulloch, U. Schollwöck, and J. von Delft, *Phys. Rev. B* **83**, 195115 (2011).
- [50] J. C. Halimeh, F. Kolley, and I. P. McCulloch, *Phys. Rev. B* **92**, 115130 (2015).
- [51] F. A. Wolf, J. A. Justiniano, I. P. McCulloch, and U. Schollwöck, *Phys. Rev. B* **91**, 115144 (2015).
- [52] H. D. Xie, R. Z. Huang, X. J. Han, X. Yan, H. H. Zhao, Z. Y. Xie, H. J. Liao, and T. Xiang, *Phys. Rev. B* **97**, 075111 (2018).
- [53] A. Dymarsky and H. Liu, *Phys. Rev. E* **99**, 010102(R) (2019).
- [54] A. E. Feiguin and S. R. White, *Phys. Rev. B* **72**, 020404(R) (2005).
- [55] C.-J. Lin and O. I. Motrunich, *Phys. Rev. Lett.* **122**, 173401 (2019).
- [56] K. Van Acoleyen, M. Mariën, and F. Verstraete, *Phys. Rev. Lett.* **111**, 170501 (2013).
- [57] B. Wouters, J. De Nardis, M. Brockmann, D. Fioretto, M. Rigol, and J.-S. Caux, *Phys. Rev. Lett.* **113**, 117202 (2014).